Embedded Selforganizing Systems

Issue Topic: "Artificial Intelligence & Machine Learning in Computer Vision Applications "

Investigation of the Cavitation Phenomenon in Centrifugal Pumps over Different Operating Flow Rates

Mohammed Khudhair Abbas
University of Diyala
Department of Mechanical engineering
Diyala, Iraq, 32001
mohammedkhudhair_eng@uodiyala.edu.iq

Abdul Salam K. Darwish
University of Bolton
Department of Civil Engineering
Bolton, UK
a.darwish@bolton.ac.uk

***Abstract*—Cavitation flow phenomena are closely linked to the design and functioning of centrifugal pumps. This phenomenon can arise in the stationary portions of the pumps or in the revolving runner-impeller. This research aimed to study cavitation behavior in a centrifugal pump at different operating flow rates: 0.5 Q, Q, 1.5 Q, and 2 Q (Q: design flow rate). The cavity formation issue can be found using a computational model (ANSYS CFX R.16). To overcome the initial cavitation, the total pressure at the inflow border gradually decreases. The novelty of this work is to accurately predict the cavitation behavior in a centrifugal pump at half time, one and a half times, and twice the designed flow rate. The calculated CFD findings indicate that high-velocity liquid is the source of bubble formation in a lower-pressure region. Cavitation initiates on the blade surface, where the leading edge and tip meet. As the NPSH decreases, the cavitation zones move from the leading edge to the trailing edge. The head-NPSH curve begins to drop as the cavity size reaches the optimum chord length of the blade.**

Keywords—Centrifugal pump, cavitation phenomenon, numerical simulation

I. INTRODUCTION

In many different sectors, liquids are transferred and distributed using pumps. Most of the time, electrical energy is used to power different kinds of pumps. Pumps serve two essential functions: moving liquids from one location to another (for example, moving water from an underground source into a storage tank) and moving liquids across a system (for example, moving lubricants through machinery and equipment) [1- 4]. Optimal pump performance is achieved by operating at high rotational speeds with minimal inlet pressure. However, this operational mode induces cavitation, leading to significant issues such as performance degradation, intense fluctuating forces on the pump components, acoustic disturbances, and material erosion [5-9]. Understanding cavitation dynamics is, therefore, essential for both design and operational efficiency. This study emphasises the necessity of investigating the causal mechanisms behind the decrease in pump heads under cavitating conditions to improve inducer designs. The research presented here delves into how cavitation influences the performance of four specific centrifugal pumps [10-16].

Due to the advancements in machinery and equipment in recent years, the issue of reducing wear has attracted much attention from researchers. This section addresses which studies were the most notable and significantly impacted the advancement of knowledge about cavitation in a centrifugal pump. Abbas, 2010 [17] computationally utilized ANSYS CFX-R_12 to determine the centrifugal pump's cavitation. The initial cavitation is initiated when the inlet total pressure is decreased by a tiny amount. Computational fluid dynamics (CFD) simulations revealed the formation of bubbles in regions of lower pressure when exposed to rapidly moving fluids. Cavitation initiates at the junction of the leading edge and tip on the blade surface. As the net positive suction head (NPSH) decreases, these cavitation zones shift from the leading edge toward the trailing edge. A notable decline in the head-NPSH relationship is observed once the cavity's length nears the maximal chord length of the blade. Akbar Toloian's 2015 study [18] delved into the dynamics of cavitation bubbles generated in fluid flow under high pressure. These bubbles are prone to abrupt collapse when the local pressure of the fluid dips below the ambient temperature's saturation vapour pressure. This collapse is precipitated by the internal pressure of the bubble being outstripped by the surrounding fluid pressure. The collapse results in bubble fragmentation upon striking rigid surfaces, a process that can be examined using laser diagnostics. Cavitation becomes a critical concern only when it leads to a reduction in pipe performance of less than 3%. Moreover, the onset of cavitation can precede this point. Noise analysis techniques are employed to predict cavitation occurrences in pump systems.

The primary reason for centrifugal pump failures is cavitation. Ranjbar et al., 2020 [19], the flow rate in a multistage centrifugal pump, without or with cavitation, is examined to assess this phenomenon. Additionally, the chance of cavitation is decreased, and the impeller's inlet condition is enhanced. This study's primary goal is to identify the optimal pump range for operation. To determine the inception cavitation zone, looking into system pump curve prediction is worthwhile. Consequently, a theoretical system

pump curve was produced using Microsoft Excel 2010; a computational fluid dynamic model was also created from the simulation findings. The start of cavitation is caused by a decrease in the NPSHa value. The main conclusions of this research are theoretical and numerical data about the effectiveness of breakdown and pump properties under various operating conditions. To prevent cavitation in pumps, the optimal operating pump range is determined to be a 330 m^3/hr flow rate.

In their 2020 study, Hongbo and colleagues [20] employed a combination of experimental approaches and numerical simulations to analyse cavitation in a Venturi tube, particularly under varying concentrations of solid mass. The numerical analysis used a two-dimensional, axisymmetric model based on computational fluid dynamics (CFD) implemented through ANSYS FLUENT 16.2, a widely recognised commercial CFD software. They introduced an innovative four-phase global model designed for more straightforward application in engineering scenarios and corroborated it with experimental data. Both the numerical and experimental results highlighted that solid particles within the cavitating Venturi tube substantially affect the cavitation process, notably intensifying it with increased solid mass concentration. The study also demonstrated that the proposed CFD model is effective and accurate at predicting cavitation dynamics and performance attributes in such settings.

The purpose of this research is to accurately predict the onset of cavitation and determine the best way to distribute the pressure field in a centrifuge pump to prevent cavitation from developing and extend the pump's lifespan.

II. RESEARCH METHODOLOGY

Turbulence modelling is essential since numerous circuits, including this flow phenomenon, can be difficult to distinguish because cavitation occurs at high Reynolds numbers. Studies show that the disturbance model for cavity flows has the best agreement with the outcomes of the experiments. As a result, this model is employed to simulate disruptions. The simulation of fluid flow using a no cavitation model is performed first. After that, it is used as a starting point for cavitation flow simulations by gradually lowering the suction pressure at the pump's input. The net positive suction head (NPSH), which is a measure of suction pressure, likewise steadily decreases. Equation 1 states that the NPSH is the difference between the pressure at the inlet and the liquid's vapour pressure [18].

$$NPSH = \frac{(P_t - P_v)}{\rho g} \tag{1}$$

where P_t is the total pressure at the inlet [Pa], P_v is the vapour pressure of the fluid [Pa], and ρ is the density of the fluid.

Cavitation refers to the process in which vapour bubbles emerge in regions of flow where the pressure is relatively low. It can be conceptualized that these vapour bubbles originate when the pressure of the liquid drops to meet or fall below its vapour pressure at the prevailing operating temperature. The static pressure of any flow is often nondimensionalized as a pressure coefficient, which is described as [18]:

$$C_p = \frac{(P - P_1)}{0.5\rho u^2} \tag{2}$$

where u is the inlet tip speed and P_1 is the inlet static pressure.

Cavitation can have a big impact on pump efficiency and performance in fluid dynamics, especially in high Reynolds number flows. This theory explains how cavitation occurs as a result of changes in inlet pressure (P_1), and how it can be predicted by pressure coefficients and flow rates.

Hospital Information technology

There are different technologies, that are already in use in a hospital setting to support the work of the doctors, workers and the management of the hospital. The intentions of these solutions are usually to collect all relevant data about the hospital patients and to create different overviews of relevant information, specially designed for separated professions and departments.

A. Flow Speeds and Pressure Coefficient

Under non-cavitating conditions, flow speeds and pressure coefficient C_p remain constant. All other pressures adjust equivalently when P_1 changes, so C_p stays the same. A given fluid velocity, geometry, and Reynolds number will result in the pressure (p) reaching its lowest point at a specific location. In this case, (p_{min}) is the differential pressure between p1 and (p_{min}):

$$C_{pmin} = \frac{(p_{min} - p_1)}{0.5\rho u^2} \tag{3}$$

where C_{pmin} is a negative quantity that depends exclusively on the value of the Reynolds number and the centrifugal pump shape.

B. Determination of Cavitation Inception

As the inlet pressure *p1* decreases, it becomes possible to determine the value of the inlet pressure (*p1*) at which cavitation initially manifests (assuming that this happens when $p_{min} = p_v$), specifically.

$$(p_1)_{\substack{cavitation \\ appearance}} = p_v + 0.5\rho u^2(-C_{p\,\min}) \tag{4}$$

The cavitation number can be calculated as follows:

$$\sigma = \frac{(p_1 - p_v)}{0.5\rho u^2} \tag{5}$$

The flow coefficient is:

$$\phi = \frac{Q}{\omega D^3} \tag{6}$$

and the head coefficient (ψ) are defined as

$$\psi = \frac{2gNPSH}{u^2} \tag{7}$$

C. Practical Implications

Understanding this relationship is essential for centrifugal pumps and other fluid systems where cavitation can cause damage and efficiency loss. To effectively avoid the detrimental effects of cavitation, engineers can design systems that operate within safe pressure ranges by accurately predicting the onset of cavitation. The extended theory indicates that the inlet pressure should be maintained above the critical threshold identified by the extended theory by choosing appropriate geometries and operational parameters and implementing control strategies for maintaining higher inlet pressures. Therefore, pressure coefficients and fluid dynamics principles are essential for predicting and mitigating cavitation in turbulent flows. Engineers can ensure hydraulic systems operating at high Reynolds numbers are reliable and

long-lasting by leveraging the relationship between inlet pressure, fluid velocity, and pressure coefficients

III. NUMERICAL MODEL

The numerical analysis utilised ANSYS CFX 16 as the computational tool. The discretisation of the Reynolds-averaged Navier–Stokes (RANS) equations was achieved through the finite volume method (FVM). A second-order model with high-resolution discretisation was preferred to ensure accurate convergence over simpler first-order methods. At 25 °C, water and vapour are the working fluids. The hub, shroud, and blade profile composed the three-dimensional geometry of the centrifugal flow pump impeller. The H-grid is applied via the flow route and blade. The RMS residuals and mass/moment imbalances were kept below 1x10-5 to ensure convergence for numerical analysis. The diameter of the impeller is 262 mm for the outer impeller and 46.3 mm for the inner impeller. Its intended operating parameters include a rotating speed of 1500 rpm, a flow rate of 200 m3/h, and a head of 20 m. The geometrical parameters for the impeller and the boundary conditions are shown in Table 1. Fig. 1 shows an isometric 3D view of the blade, hub, shroud, and mesh elements at 50% span. The rotating frame of reference is used to carry out the flow simulation. The turbulence is represented by the k-ω SST model. The cavitation model with the volume of fluid model is chosen for turbulence wall treatments. The solution scheme uses the upwind difference. The total elements and nodes utilised in the computational domain were 209374 and 97901, respectively.

IV. RESULTS

Prior to investigating the cavitation phenomenon, the experimental data of Reference (3) are used to verify the accuracy of the numerical analysis. Using reference (3), Fig. (2) validates the numerical analysis using the head coefficient and cavitation characteristics. It is evident that the results for various operational flow rates were 3-7% higher than the experimental results due to the numerical analysis failure to account for mechanical loss, leakage, and roughness. The inlet and outflow of the numerical analysis were designed with a straight flow route, whereas the experimental setup uses complexly curved pipes along the closed loop. The head

TABLE 1. THE GEOMETRIC PARAMETERS AND BOUNDARY CONDITIONS FOR THE IMPELLER FOR (Q: DESIGN FLOW RATE).

Impeller dimension		**Boundary condition**	
Inlet diameter of impeller (mm)	46.3	Blade number, Z	6
Outlet diameter of impeller (mm)	262	Rotational speed	2400 rpm
Outlet width b2 (mm)	36.4	Volume flow rate	$200m^3/h$
Blade inlet angle at hub β1 h (°)	19.77	Density	$1000kg/m^3$
Blade inlet angle at tip β1t (°)	27.62	Head rise	20 m
Blade outlet angle β2 (°)	13.10		
Inlet flow angle	90 °		

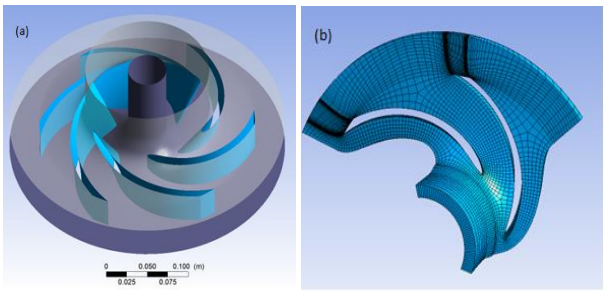

Fig. 1. The computational domain of the centrifugal pump and b mesh elements at 50% span

performance curve displays a cusp shortly before breakdown because head degradation begins at flow coefficients smaller than the design value, or approximately 0.5 Q. This is because the cavitation number further decreases at these flow coefficients. A slight increase in head size at moderate cavitation intensity levels is evident in the head-drop characteristics at 1.5 Q and 2 Q; Friedrich et al. [21] previously reported similar characteristics.

To examine the impact of cavitation on centrifugal pumps, many characteristics, such as the total pressure (Pt) and relative total pressure (Ptr), were taken into account at the leading and trailing edges of the blades of the centrifugal pumps. Figs. 3 and 4 show the mass average of Pt and Ptr on the meridional surface at different flow rates. With each flow rate, the suction pressure steadily decreases. The net positive suction head (NPSH) decreases as a result of decreased suction pressure. Low-pressure zones emerge, and vapour bubble production starts when the NPSH falls below a particular threshold. These figures illustrate the corresponding total pressure on the suction and pressure surfaces of the impeller blade at various flow rates. These contours are displayed for the downstream impeller. Since the relative total pressure is the sum of the static pressure and the dynamic head, depending on the relative velocity, it accurately depicts the flow dynamics inside a rotor. A gradient of pressure forms from the hub to the shroud as a result of the flow shifting from an axial to radial orientation. Figs. 5–8 show the contours of Pt and Ptr at the leading and trailing edges of the blades of the centrifugal pumps at different flow rates, respectively. The maximum Pt and Ptr occur in the case of 0.5 Q and decrease gradually to 2 Q. The fluid flow impacts at the leading and trailing form edges are presented. At the very least, the pressure is apparent close to the attack suction edge (see Figures 5 and 6). The leading edge, which is also the suction side, is where flow splitting occurs and contributes to this

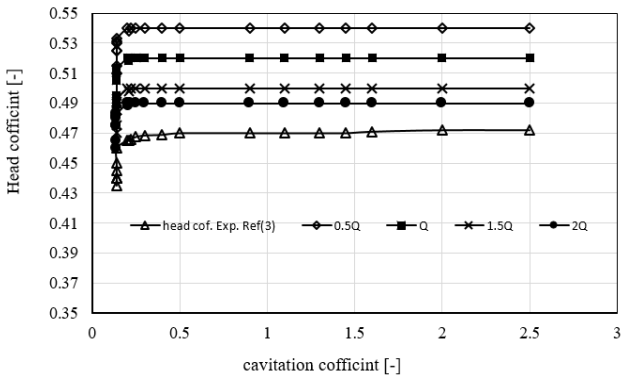

Fig. 2. Comparison of experimental and computational results with respect to the head coefficient and cavitation characteristics at different operating flow rates.

splitting. Figs. 7 and 8 show similar variations at the trailing edge. The flow becomes extremely tangential to the shroud at the design flow rate. The flow encounters the blade's upper convex surface rather than the leading edge due to the small flow angle near the shroud.

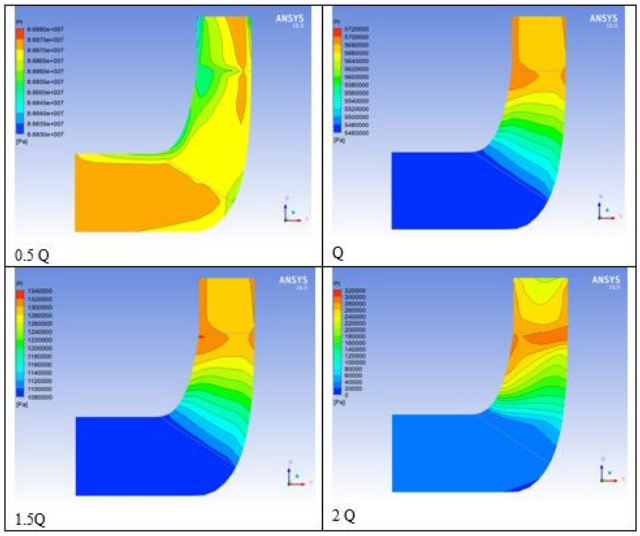

Fig. 3. Contours of mass-averaged P_t on the meridional surface at different operating flow rates.

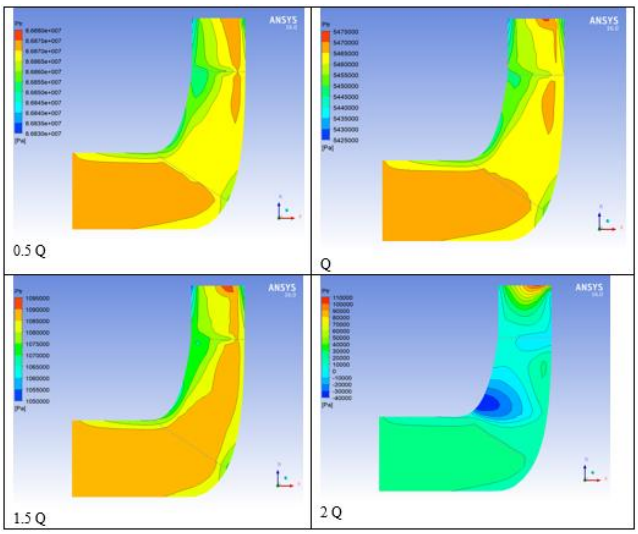

Fig. 4. Contours of mass-averaged Ptr on the meridional surface at different operating flow rates.

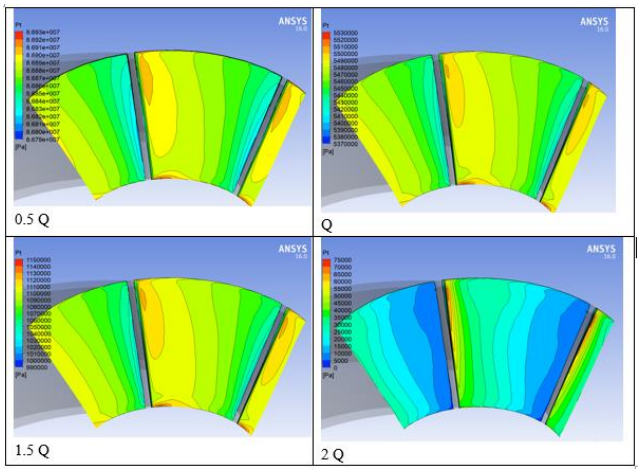

Fig. 5. Contours of Pt at blade LE at different operating flow rates.

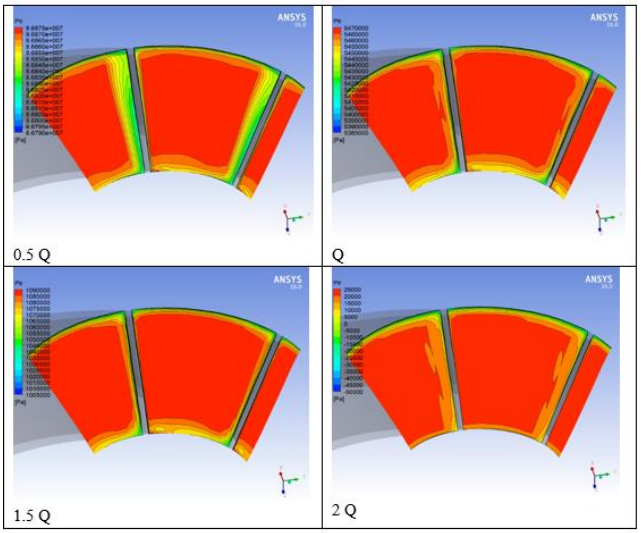

Fig. 6. Contours of Ptr at blade LE at different operating flow rates.

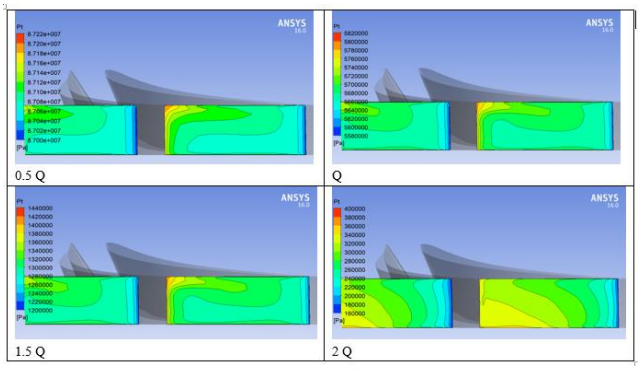

Fig. 7. Contour of Pt at blade TE at different operating flow rates.

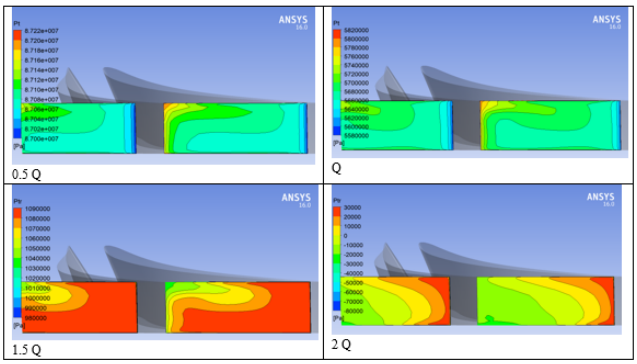

Fig. 8. Contours of Ptr at blade TE at different operating flow rates.

Figs. 9–11 demonstrate the distributions of pressure along 20%, 50%, and 80% of the blades span at different flow rates. It can be noticed that the values of pressure are maximum at trailing edges for all cases, compared with these values at leading edges for the same flow rate. When compared with the same span of 20%, it can be noticed that the pressure value is high in the 0.5 Q case and minimal in the 2 Q case (see Fig. 9). This tendency is evident for all the other spans in Figs 10 and 11. The streamwise positions of every span between the LE and TE are normalized to 0 and 1, respectively. The distributions of the total pressure and static pressure (Ps) at different flow rates are shown in Fig. 12. The total pressure is higher than the static pressure. Fig. 12 highlights the effect of the cavitation phenomenon on the blade. The load on the pressure and suction sides of the blade at small flow rates indicates that there is absolutely no vapour bubble or

cavitation. The decrease in the suction head encourages the creation of bubbles, which consume a large amount of liquid water and stop the impeller and liquid water from transferring energy to one another. The static pressure on the blade surface deteriorates in the Q and 1.5Q cases. The pump with the largest flow rate collapses during blade loading. The impeller cannot propel the liquid because there is no load on the blade inside half of the blade length. In this scenario, the pump exhibits severe cavitation, with many bubbles clogging the flow channels and causing abnormal behavior and extremely low efficiency. Fig. 3 and 4 predict and discuss this fantastic reversal effect.

The relative velocity distributions in suction, pressure, and blade midpoint at different operating flow rates are also displayed in Fig. 13. The blade output is where the most significant flow rate increase from the input to the output occurs. More pressure is required on the suction surface to pressurise the fluid at the edge of the pressure attack. Because of this pressure distribution, the relative velocities at the suction surface seem considerably greater than those at near-surface pressure levels. A thorough comprehension of cavitation processes can be obtained by plotting the circumferentially mass-averaged blade and flow angles (Fig. 14).

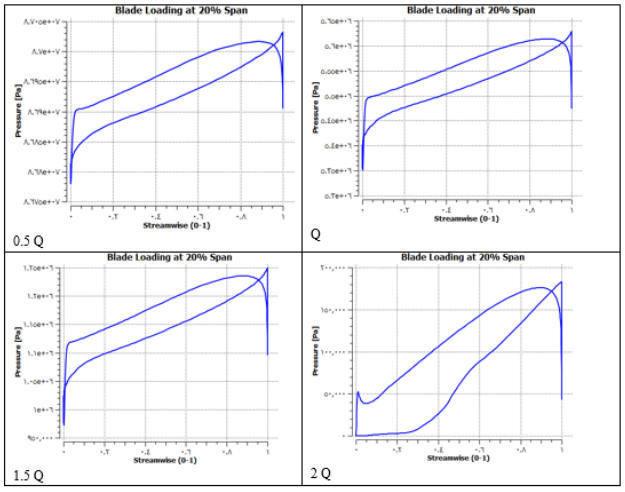

Fig. 9. Distribution of pressure at 20% span at different operating flow rates.

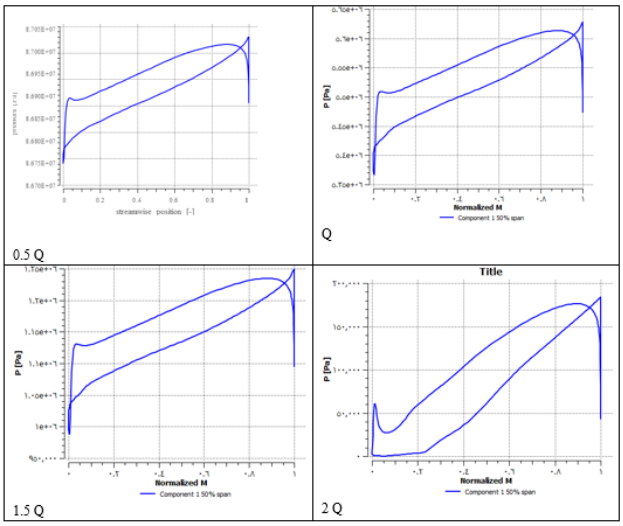

Fig. 10. Distribution of pressure at 50% span at different operating flow rates.

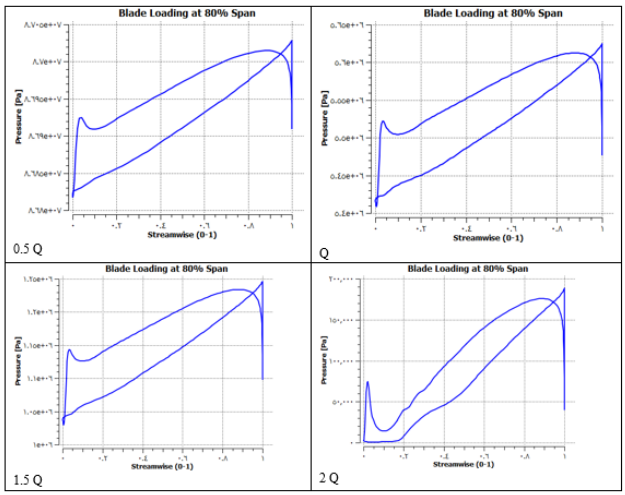

Fig. 11. Distribution of pressure at 80% span at different operating flow rates.

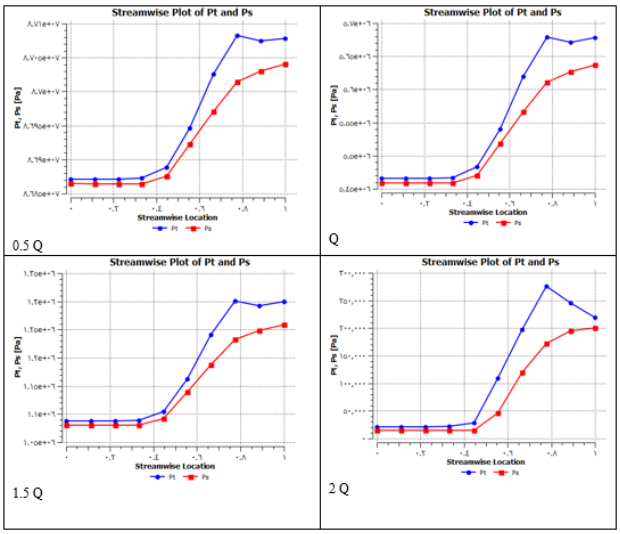

Fig. 12. Distribution of Pt and Ps at different operating flow rates.

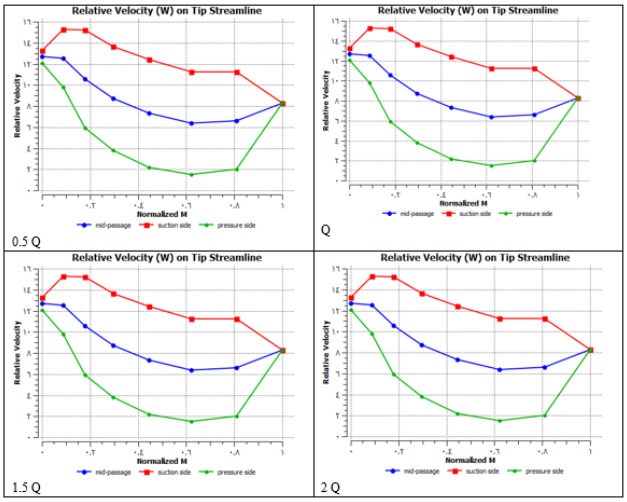

Fig. 13. Throughflow: Relative velocity (W) on the tip streamline at different operating flow rates.

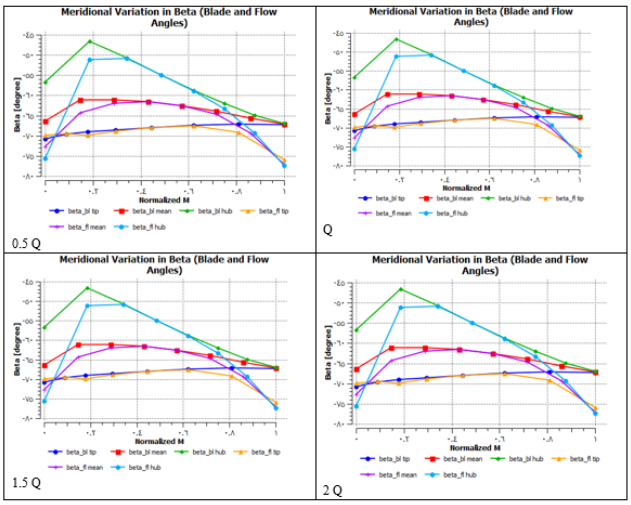

Fig. 14. Circumferentially mass averaged blade and flow angles at different operating flow rates.

V. CONCLUSION

This article explored the relationship between cavitation occurrence and flow rates in centrifugal pumps, offering a detailed numerical analysis and contrasting it with experimental results. The study revealed that cavitating flow patterns vary with flow rate. Specifically, cavities are uniformly distributed across each blade at higher flow rates, whereas lower flow rates result in asymmetrical blade cavitation, concentrating cavitation intensity along specific blade paths. The key findings include the following:

1. At flow rates lower than half the design rate, the head-drop profiles exhibit a distinct encroaching shape prior to collapse. Conversely, a pronounced head drop is observed at flow rates such as 1.5 or 2 times the design rate. The study also noted that cavity shapes expand with decreasing inlet pressure, with similar cavity morphologies occurring at lower flow rates. There is a clear distinction in the cavitation characteristics of centrifugal pumps between high and low flow rates.
2. Flow visualization techniques confirmed that at high flow rates, the cavitation patterns align with the predictions of numerical models, exhibiting gradual head-drop curves and asymmetrical cavitation on the blades.
3. The likelihood of cavitation increases significantly at flow rates higher than the design rate. Operating the pump at 1.5 or 2 times the design flow rate at the same net positive action head (NPSH) heightens the risk of vapour formation and cavitation compared to running it at the design or half the design flow rate.

Finally, the strong agreement between the numerical and experimental results in this study validates the accuracy of the proposed numerical model in replicating the spatial flow patterns in simulated pumps. Consequently, this research provides valuable insights for analyzing, understanding, and managing cavitation dynamics in centrifugal pumps. Additionally, the findings related to the influence of the blade entry angle on cavitation offer practical guidance for centrifugal pump design in industrial applications, particularly in scenarios involving high or low flow rates.

Conflict of interest: The authors have no conflicts of interest to disclose regarding this paper's study, writing, or publication.

Availability of data and materials: All the data presented in this article are available.

Competing interests: The author has no relevant financial or nonfinancial interests to disclose.

Funding: No funding was found for this article.

ACKNOWLEDGEMENTS

The authors would like to thank Eng. Husam S. Mansor, University of Diyala–Diyala, Iraq, for helping us complete this work.

NOMENCLATURE

P_1	inlet static pressure [Pa]	C_p	pressure coefficient
P_t	Total pressure at the inlet [Pa]	σ	cavitation number
P_{tr}	Relative Total pressure	ρ	the density of the fluid [kg/m³]
P_v	the vapour pressure of the fluid [Pa]	ψ	head coefficient
NPSH	Net positive section head	CFD	Computational Fluid Dynamics
U	upstream mean velocity [m/s]	LE	leading edges of blades
Q	the flow rate [m³/h]	TE	Trailing edges of blades
ϕ	flow coefficient	Z	the number of blades

REFERENCES

[1] N. Dhote, Y. Waykar & M. Khond, "Numerical and cavitation analysis of a centrifugal pump", Proceedings of Conference on Advances on Trends in Engineering Projects (nctep-2019), in association with novateur publications IJIERT-ISSN no: 2394-3696, (2019).

[2] M. Sathasivam,. J. Thaarrini, N. Sarath Kumar & S. J. Sanjeykumaran Review on cavitation analysis in pipes, international journal of civil engineering and technology (ijciet), (2018), volume 9, issue 10, pp. 1231–1238.

[3] Yong K., Hyeon Y., Jun S., Sung K., Kyoung L. & Young C " Numerical study on the cavitation phenomenon for the head drop and unsteady bubble patterns with a difference in the incidence angle of a mixed-flow pump", Advances in Mech. Eng. (2020), Vol. 12(4) 1–18, https://doi.org/10.1177/1687814020914790.

[4] Georgios M., Ioannis K., George A. & Ioannis A. "Numerical simulation of the performance of a centrifugal pump with a semi open impeller under normal and cavitating conditions", applied mathematical modelling, (2021), 89 ,1814–1834, https://doi.org/10.1016/j.apm.2020.08.074

[5] Bao N. & Jun K. " Numerical analysis on the cavitation performance of a seawater cooling pump", journal of the Korean society of marine environment & safety, vol. 25, no. 1, (2019), pp. 130-137, February 28, https://doi.org/10.7837/kosomes.2019.25.1.13

[6] O. Delghosa, R. Patella, J. Reboud & B. " Pouffary 3D numerical simulation of pump cavitating behavior". ASME FEDSM, (2019), https://doi.org/10.1115/FEDSM2002-31188.

[7] O. Delgosha, R. Patella & J Reboud, A Numerical Model to Predict Unsteady Cavitating Flow Behavior in Inducer Blade Cascades, Fifth International Symposium on Cavitation Osaka, Japan(CAV2003), https://doi.org/10.1115/1.2409320

[8] M. Hofmann, B. Stoffel, O. Delgosha, R. Patella & J. Reboud, " Experimental and Numerical Studies in A Centrifugal Pump With two-Dimensional curved blades in Cavitating Condition" , Transactions of The Asme, (2003)Vol. 125 CAV2001:sessionB7.005.

[9] Qiaorui Si, Asad Ali, Minquan Liao, Jianping Yuan, Yuanyuan Gu, Shouqi, Yuan & Gerard Bois " Assessment of Cavitation Noise in A Centrifugal Pump Using Acoustic Finite Element Method and Spherical Cavity Radiation Theory", Engineering Applications of Computational Fluid Mechanics, (2023) Vol. 17, No. 1, 2173302, 10.1080/19942060.2023.2173302

[10] Mohammed KH., Yasseen A. & Sami A.(2021), Flame behaviour and flame location in large-eddy simulation of the turbulent premixed combustion, Energy 232, 121067. https://doi.org/10.1016/j.energy.2021.121067.

[11] Mohammed KH.,Yahya, S.G.& Al-Rubaiy, (2020) , Experimental and Computational Investigation of Flame Holders in Combustion Chambers at Different Thermal Loads, journal of Thermal Engineering, (6), pp. 369–378.

[12] Yanxia Fu, Jianping Yuan, Shouqi Yuan & Giovanni Pace, Numerical And Experimental Analysis Of Flow Phenomena In A Centrifugal Pump Operating Under Low Flow Rates, Journal Of Fluids Engineering, January 2015, Vol. 137. https://doi.org/10.1115/1.4027142

[13] Almahdawi, Y., Kh Abbas, M., Al-Samari, A. & Aldabash, N.. "Temperature effect in the energy degradation of photovoltaic power system". Journal of Thermal Engineering, (2023) *9(5), 1153-1162.* https://doi.org/10.18186/thermal.1370726.

[14] D. Sébastien , Olivier & Dazin), "X-ray Measurements in A Cavitating Centrifugal Pump During Fast Start-Ups". Journal of Fluids Engineering, *, (2013Vol. 135*, htpp://doi.org//10.1115/1.4023677

[15] S. Anish " Study of Secondary Flow Modifications at Impeller Exit of a Centrifugal Compressor", Open Journal of Fluid Dynamics, *,(2012* 2012, 2, 248-htpp://doi.org//10.4236/ojfd.2012.24A029

[16] H. Shi, M. Li, P. Nikrityuk, & Q. Liu, "Experimental and numerical study of cavitation flows in venturi tubes": From CFD to an empirical model," Chem. Eng. Sci., vol. 207, pp. 672–687, 2020, htpp://doi.org//10.1016/j.ces.2020.07.004.

[17] H. Patil), "Detection, Causes And Ways Of Prevention Of Cavitation In Pumps", International Journal of Engineering Applied Sciences and Technology (2021 doi.org//10.33564/IJEAST.2021.v06i03.011

[18] Ranjbar B., M. Ehghaghi, & F. Ranjbar, "" The study of cavitation phenomenon in multistage centrifugal pump and reduction of its damages" ," Sci. Iran., vol. 27, no. 3 B, pp. 1339–1348, 2020, htpp://doi.org//10.24200/SCI.2019.52112.2539.

[19] Hongbo Shi, Mingda Li, Qingxia Liu& Petr Nikrityuk, " Experimental and numerical study of cavitating particulate flows in a Venturi tube", Chemical Engineering Science,) (2020Vol. 219, 29, https://doi.org/10.1016/j.ces.2020.115598

[20] Friedrichs, J., & Kosyna, G., " Rotating Cavitation in a Centrifugal Pump of Low Specific Speed" , ASME J. Fluids Eng., (2002) 124, pp. 356–362, https://doi.org/10.1115/1.1457451.